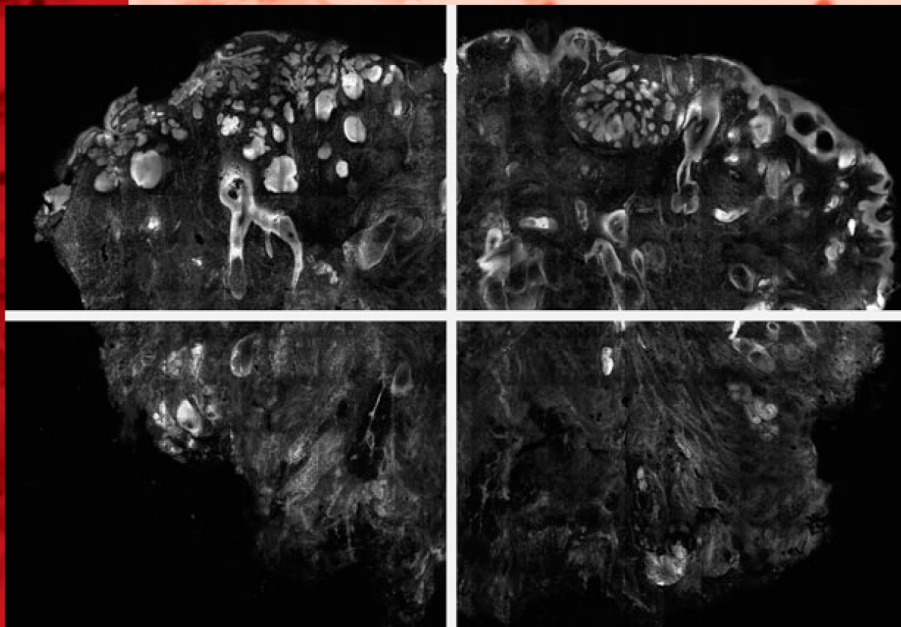


VOLUME 160 | NUMBER 6 | JUNE 2009



BJD

British Journal of Dermatology

*Published for
the British Association of Dermatologists
by Blackwell Publishing*

issn: 0007-0963

<http://www.blackwellpublishing.com/bjd>

 WILEY-
BLACKWELL

Detection of basal cell carcinomas in Mohs excisions with fluorescence confocal mosaicing microscopy

J.K. Karen, D.S. Gareau, S.W. Dusza, M. Tudisco, M. Rajadhyaksha and K.S. Nehal

Dermatology Service, Memorial Sloan-Kettering Cancer Center, New York, NY 10022, U.S.A.

Summary

Correspondence

Kishwer S. Nehal.

E-mail: nehalk@mskcc.org

Accepted for publication

21 January 2009

Key words

basal cell carcinoma, confocal microscopy

Conflicts of interest

M.R. is a former employee of Lucid Inc., the company that makes and sells the VivaScope confocal microscope. He owns equity in Lucid. The VivaScope is the commercial version of an original laboratory confocal microscope that was developed by M.R. when he was in the Department of Dermatology at Massachusetts General Hospital, Harvard Medical School.

J.K.K. and D.S.G., and M.R. and K.S.N. (senior two authors) contributed equally to this manuscript.

DOI 10.1111/j.1365-2133.2009.09141.x

Background High-resolution real-time imaging of human skin is possible with a confocal microscope either *in vivo* or in freshly excised tissue *ex vivo*. Nuclear and cellular morphology is observed in thin optical sections, similar to that in conventional histology. Contrast agents such as acridine orange in fluorescence and acetic acid in reflectance have been used in *ex vivo* imaging to enhance nuclear contrast.

Objectives To evaluate the sensitivity and specificity of *ex vivo* real-time imaging with fluorescence confocal mosaicing microscopy, using acridine orange, for the detection of residual basal cell carcinoma (BCC) in Mohs fresh tissue excisions.

Methods Forty-eight discarded skin excisions were collected following completion of Mohs surgery, consisting of excisions with and without residual BCC of all major subtypes. The tissue was stained with acridine orange and imaged with a fluorescent confocal mosaicing microscope. Confocal mosaics were matched to the corresponding haematoxylin and eosin-stained Mohs frozen sections. Each mosaic was divided into subsections, resulting in 149 submosaics for study. Two Mohs surgeons, who were blinded to the cases, independently assessed confocal submosaics and recorded the presence or absence of BCC, location, and histological subtype(s). Assessment of confocal mosaics was by comparison with corresponding Mohs surgery maps.

Results The overall sensitivity and specificity of detecting residual BCC was 96.6% and 89.2%, respectively. The positive predictive value was 92.3% and the negative predictive value 94.7%. Very good correlation was observed between confocal mosaics and matched Mohs frozen sections for benign and malignant skin structures, overall tumour burden and location, and identification of all major histological subtypes of BCC.

Conclusions Fluorescent confocal mosaicing microscopy using acridine orange enables detection of residual BCC of all subtypes in Mohs fresh tissue excisions with high accuracy. This observation is an important step towards the long-term clinical goal of using a noninvasive imaging modality for potential real-time surgical pathology-at-the bedside for skin and other tissues.

There is growing interest in rapid noninvasive imaging of skin cancers with optical imaging technologies such as Raman spectroscopy,^{1,2} fluorescence polarization,³ multiphoton,^{4,5} fluorescence lifetime,⁶ fluorescence imaging,^{7,8} optical coherence tomography⁹ and reflectance confocal microscopy.¹⁰ Reflectance confocal microscopy has made important strides towards clinical applications with high resolution and sectioning comparable with that of conventional histology. Nuclear and cellular detail is noninvasively imaged in thin optical sections (1–5 µm) with high lateral resolution (0.2–1.0 µm) and high contrast, using objective lenses with high numerical

apertures (NAs) of 0.7–1.4 and magnifications of 20–100 ×. Recent studies have demonstrated excellent correlation between confocal images and histopathology for normal skin and benign and malignant lesions *in vivo* and in freshly excised tissue *ex vivo*.¹⁰

Confocal microscopes typically display small fields-of-view of 0.2–1.0 mm, given the need for high NAs and the corresponding use of high magnification lenses. For examination of large areas of tissue, we developed a confocal mosaicing microscope.^{11–15} A two-dimensional array of images is acquired and stitched together in software, to create a mosaic

that displays a large field-of-view. In our current laboratory microscope, a field-of-view of up to 12 × 12 mm may be displayed,^{13–15} which is equivalent to 2 × magnification that is routinely used when examining pathology.

In previous research, we demonstrated the feasibility of *ex vivo* imaging of skin excisions from Mohs surgery with confocal mosaicing microscopy.^{13–15} Superficial, nodular and micronodular basal cell carcinomas (BCCs) were visually detected in reflectance mode, using acetic acid as a contrast agent (i.e. acetowhitening) to brighten nuclei. However, infiltrative BCCs, which tend to be smaller in size and deeper in the dermis, were not consistently detected. In the reflectance mode, the acetowhitened nuclei as well as the surrounding normal dermis strongly backscatter light. Therefore, large and densely nucleated tumours are detected, whereas small and sparsely nucleated tumours remain obscured within the deeper dermis.

More recently, fluorescence has shown stronger enhancements between nuclear and dermal contrast and improved detection of tumours.^{15,16} Compared with scattering in reflectance, endogenous autofluorescence from the dermis is relatively weak under real-time high-resolution confocal imaging conditions. With a contrast agent that stains nuclei, fluorescent light emission may be collected specifically from nuclear morphology with very little from the surrounding dermis, resulting in 1000-fold improvement in nuclear-to-dermal contrast.¹⁵ The efficacy of fluorescence using methylene blue and toluidine blue for the detection of BCCs in Mohs excisions was first shown by Al-Arashi *et al.*¹⁶ Subsequently, we showed that another well-known contrast agent for nuclei, acridine orange, also strongly enhances nuclear-to-dermal contrast and allows detection of all subtypes of BCC, including infiltrative tumours.¹⁵ Importantly, use of acridine orange does not affect any subsequent frozen pathology.¹⁵

The aim of this study was to evaluate the accuracy of fluorescence confocal mosaicing microscopy using acridine orange for the detection of residual BCC in Mohs fresh tissue excisions. This is another important step towards the long-term goal of developing and potentially using confocal microscopy as a noninvasive imaging tool for real-time surgical pathology-at-the bedside in skin and other tissues.

Materials and methods

Tissue collection and preparation

This study was conducted in the Mohs Surgery Unit at Memorial Sloan-Kettering Cancer Center (New York, NY, U.S.A.). Mohs surgery was performed according to standard procedure: tissue excised, divided, inked, processed by frozen sections, stained with haematoxylin and eosin (H&E) and evaluated by conventional light microscopy. Following completion of the Mohs surgery for biopsy-proven BCCs, excess tissue was collected for confocal imaging under Institutional Review Board-approved protocol. The excess tissue represented the remnants of the excisions that are routinely discarded, such

that our research did not interfere with the routine Mohs surgical procedure or affect patient care.

The fresh frozen tissue was thawed, rinsed with isotonic saline, immersed in 1 mmol L⁻¹ acridine orange (pH 6.0) for 20 s, rinsed with isotonic saline again to remove excess unbound contrast agent, and then imaged with the confocal mosaicing microscope. Details of the experimental study, to develop optimum staining with acridine orange, were previously reported.¹⁵

Acridine orange provides strong and robust nuclear-to-cytoplasm and nuclear-to-dermis contrast.¹⁵ The fluorescence is resistant to photobleaching during the mosaicing process. With illumination power of 3–5 mW on the tissue, the time for fluorescence bleaching was determined to be ~3 min. This is on the same order of magnitude as ~1 min, as reported elsewhere but under different conditions.¹⁷

Fluorescence confocal mosaicing microscopy

Confocal mosaics were acquired using a modified laboratory version of a commercial confocal laser scanning microscope (VivaScope 2000; Lucid Inc., Rochester, NY, U.S.A.). The instrumentation and imaging details have been described previously.^{12–15} In brief, an argon-ion laser at a wavelength of 488 nm illuminated tissue with low power of 5 mW. Fluorescence emission was detected in the range 500–600 nm. A specially engineered tissue fixture was used for mounting Mohs surgical excisions. The design and operation of the tissue fixture simulates that of the mount in cryostats that are used for preparing frozen sections. A two-dimensional array of images was captured using a 30 ×, 0.9 NA custom-designed water immersion objective lens (StableView; Lucid Inc.). The lens provides a field-of-view of 0.43 mm, with optical sectioning of ~1 μm and lateral resolution of ~0.25 μm. Only the exposed or cut surface of the discarded excision was imaged. This exposed surface corresponds to the surgical margin seen on Mohs frozen sections. Following image acquisition, no additional processing of the confocal images was performed.

The images were seamlessly stitched together to create a confocal mosaic, or a map of the entire excision, with a Matlab-based software algorithm (MathWorks, Natick, MA, U.S.A.). The mathematics of the algorithm is detailed in our previous work.^{14,15} In our current laboratory system, up to 36 × 36 images may be stitched together to display a field-of-view of up to 12 × 12 mm. This field-of-view is equivalent to that seen with light microscope magnification of 2 ×. Acquiring the array of images and creating a mosaic currently requires up to 9 min. The entire mosaic displays a low-resolution map at low magnification, showing the overall location and morphology of skin. Additionally, smaller portions called submosaics display cellular and nuclear detail at higher magnification and higher resolution.

An entire mosaic consists of 23 040 × 17 280 pixels and requires 325 MB of memory. The mosaics were scaled down, resulting in lateral resolution and display pixelation that were equivalent to that in a 2 × view of pathology. The final mosaic

consists of approximately 2500×1900 pixels with lateral resolution of $\sim 4 \mu\text{m}$ and requires only 4 MB of memory.^{13–15} The mosaics were viewed on a 30-inch flat-screen monitor (Dell 222-7175 with a GeForce 880 GTS video card) with 2500×1900 pixels. With digital zooming, submosaics were also observed. For example, while an entire mosaic displays with $2 \times$ magnification, a quarter submosaic displays with $4 \times$.

Study sample and design

Forty-eight confocal mosaics were prepared for the study. These represented a convenience sample of excisions that were from both positive (i.e. residual BCC) and negative (i.e. no residual BCC) Mohs stages. This sample was enriched to include all major subtypes of BCCs (i.e. superficial, nodular, micronodular and infiltrative).

An experienced Mohs histotechnician (M.T.) and an engineer (D.S.G.) reviewed all mosaics for overall image quality and visually correlated them to the corresponding H&E-stained Mohs frozen sections, to confirm that concordant mosaics and pathology were being compared. Small distortions in the imaged surface of the tissue often occur due to the thawing, staining and rinsing process and after mounting into the fixture. Confocal mosaics were therefore expected to show close (but not necessarily exact) correlation to the corresponding Mohs frozen section. Three mosaics were eliminated from the study due to poor image quality or poor correlation to frozen pathology, resulting in 45 mosaics that were assessed.

The Mohs tissue pieces ranged in size from 5 to 20 mm. Each confocal mosaic (which displays at $2 \times$ magnification) was divided into two to four smaller submosaics, depending on tissue size (Fig. 1). Accordingly, the study sample comprised 149 submosaics of which 89 (59.7%) contained residual BCC and 60 (40.3%) contained no residual BCC. The histological subtypes of BCC in the 89 cases were: 38 mixed histology, 22 nodular, 12 infiltrative, 10 micronodular and seven superficial.

Two Mohs surgeons (K.S.N., J.K.K.), who were blinded to case status, independently assessed the 149 submosaics (total sample number 298) during four sessions over a period of 1 month. Confocal submosaics were presented in a random order at $4 \times$ magnification. To mimic the standard examination of pathology, digital zooming up to a maximum magnification of $30 \times$ was permitted. For each submosaic, each Mohs surgeon recorded the presence or absence of BCC, documented tumour location on a map similar to that routinely drawn during Mohs surgery, recorded the histological subtype(s) and commented on the image quality.

Statistical analysis

The outcome variable in this study was the assessment of presence or absence of BCC tumour in each of the submosaics. This assessment was compared with the 'gold standard' which is the Mohs maps that were drawn by the Mohs surgeon

(K.S.N.) at the time of surgery. Measures of detection accuracy were estimated using binary marginal general linear models. When there were discordant cases (i.e. one or both observers' assessment did not match the Mohs map), submosaics and the corresponding Mohs frozen section were reviewed by both Mohs surgeons (K.S.N., J.K.K.) and an engineer (D.S.G.) to assess the source of discordance. All statistical analyses were performed in STATA SE v.9.2 (StataCorp, College Station, TX, U.S.A.).

Results

Detection accuracy

The accuracy of fluorescence confocal mosaicing microscopy for the detection of residual BCC or absence of BCC in Mohs fresh tissue excisions was very good. Of the 60 true negatives, 50 and 57 were correctly diagnosed by observers 1 and 2, respectively (Fig. 2a,b). Of the 89 true positives, 88 and 84 were correctly diagnosed by observers 1 and 2, respectively (Fig. 2c,d). Table 1 details the sensitivity, specificity, positive predictive value and negative predictive value of each observer and the overall performance. There was no statistical difference in detection accuracy between the two observers.

Review of the discordant cases showed various sources of error. The initial four missed cases were a result of a learning curve or lack of confidence in evaluating confocal images. There was a trend towards improved sensitivity and specificity for both observers as the study progressed, consistent with a learning curve. Other causes of error were technical issues such as confocal artifact in two cases (saturation of contrast dye or illumination mimicking the appearance of a tumour focus) and poor tissue integrity altering tumour presentation in four cases (missed superficial BCC when the epidermal margin was not complete). True histological interpretation errors occurred in eight cases (differentiating miniaturized hair follicle from BCC and BCC being obscured by dense inflammation). Of the false-negative errors, none involved infiltrative BCCs (two nodular; two micronodular; two superficial).

Qualitative assessment

The examination of confocal mosaics and submosaics mimics the viewing of frozen pathology – rapid examination at low resolution of a wide field-of-view aided, as needed, by further high-resolution inspection of nuclear morphology in smaller fields-of-view. Viewing mosaics at low magnification of $4 \times$ was usually sufficient to readily detect and distinguish residual nodular and micronodular BCC from surrounding benign structures and dark dermis, based on the relatively strong fluorescence signal (brightness and contrast), large tumour morphology and nuclear atypia (Fig. 2c,d). Questionable or suspicious areas, such as a small focus of superficial (Fig. 3) or infiltrative BCC (Fig. 4) or tissue with dense inflammation, were further delineated at higher magnification of up to $30 \times$, allowing assessment of individual nuclear detail. Digital

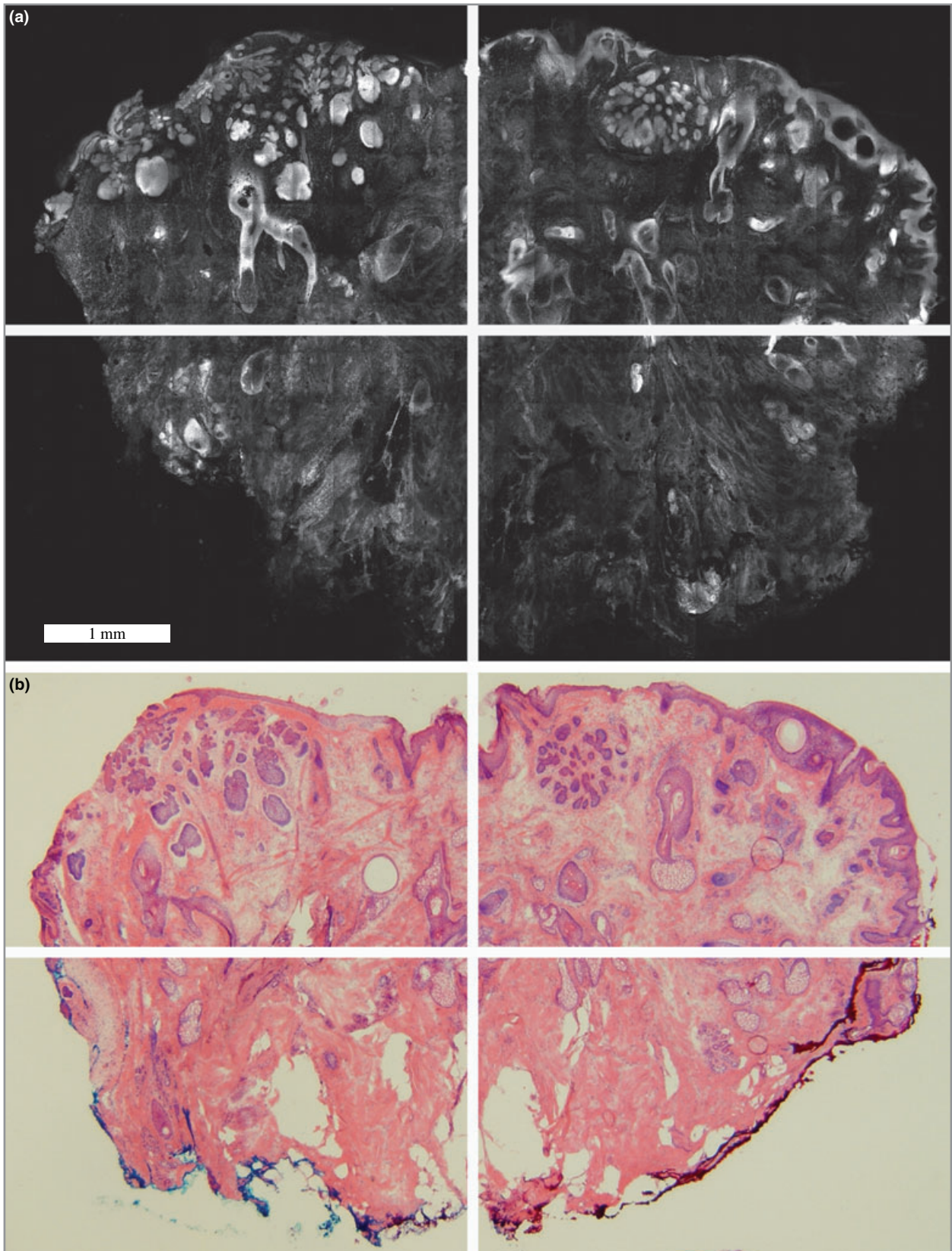


Fig 1. Study design. Fluorescent confocal mosaic (a) and corresponding haematoxylin and eosin-stained Mohs frozen section (b) at a magnification of 2 ×. Each is divided into four quadrants, as indicated by the white lines. Each quadrant represents a submosaic presented for study.

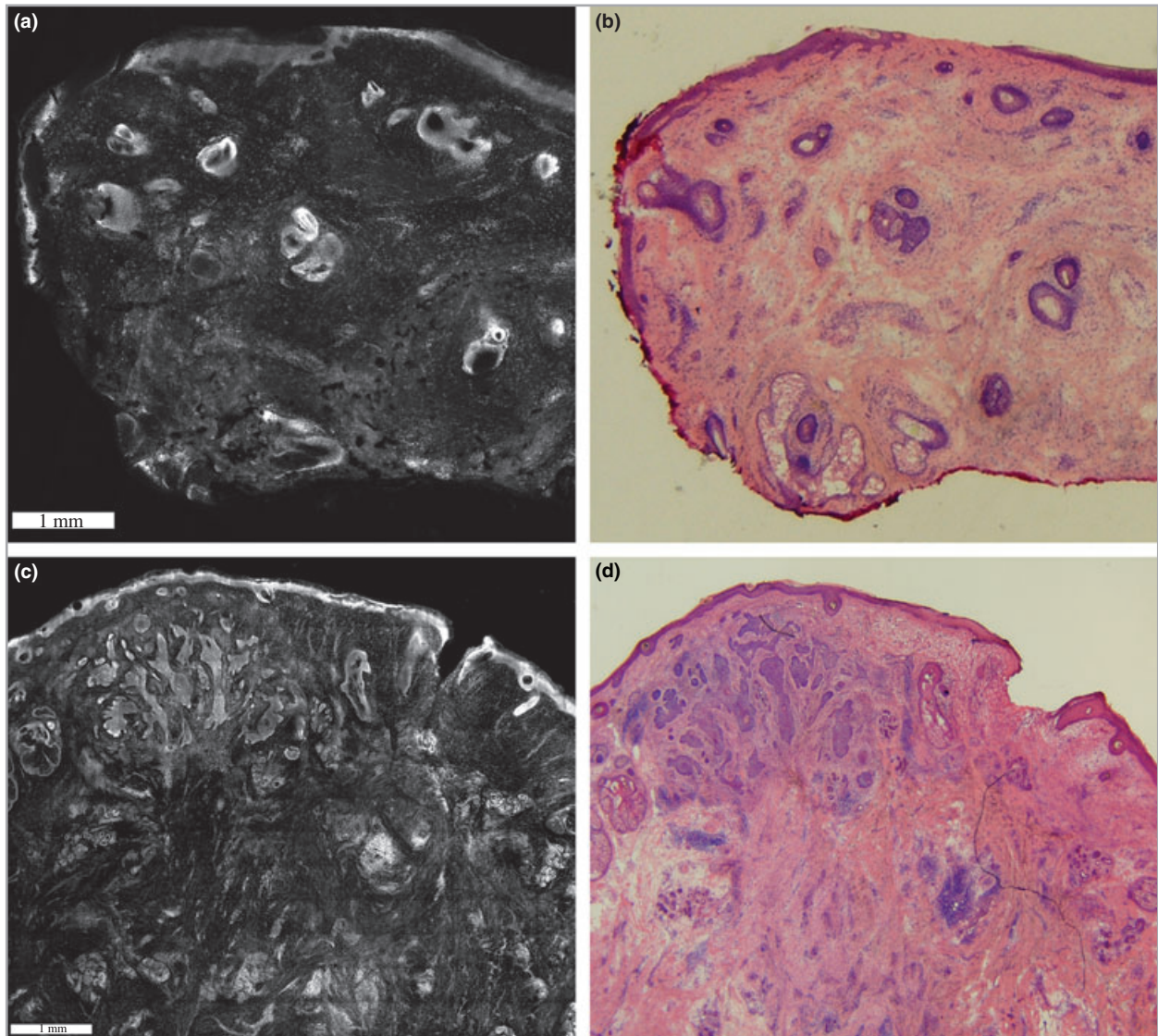


Fig 2. Fluorescent confocal submosaics (a, c) and the corresponding haematoxylin and eosin-stained Mohs frozen sections (b, d) at $4\times$ magnification. The submosaic and frozen section of a negative Mohs stage shows no residual basal cell carcinoma (BCC) (a, b); positive Mohs stage shows residual BCC within upper dermis (c, d). There is good correlation between the mosaics and the corresponding frozen sections with respect to the overall size, shape, location and morphology of benign and malignant skin structures.

	Overall, %	95% CI	Observer 1 (expert), %	Observer 2 (novice), %	P-value ^a
Sensitivity	96.6	92.8–98.7	98.9	94.4	0.10
Specificity	89.2	82.2–94.1	83.3	95.0	0.06
PPV	92.3	88.3–96.2	89.8	96.5	0.08
NPV	94.7	88.8–98.0	98.4	91.9	0.19

^aP-value is for the difference in sensitivity, specificity, PPV and NPV between observers. CI, confidence interval; PPV, positive predictive value; NPV, negative predictive value.

Table 1 Accuracy of detecting basal cell carcinomas with fluorescence confocal mosaicing microscopy, using acridine orange. The measures are shown for each observer as well as overall performance

zooming at $30\times$ magnification was equivalent to viewing individual images within a mosaic. However, such zooming and the use of magnification higher than $4\times$ were rarely performed. The image quality of the mosaics was good in the

majority of cases. Correlation was good between the maps drawn from the confocal submosaics and the corresponding Mohs maps from the frozen pathology, for overall tumour burden, location and morphology of BCC tumour.

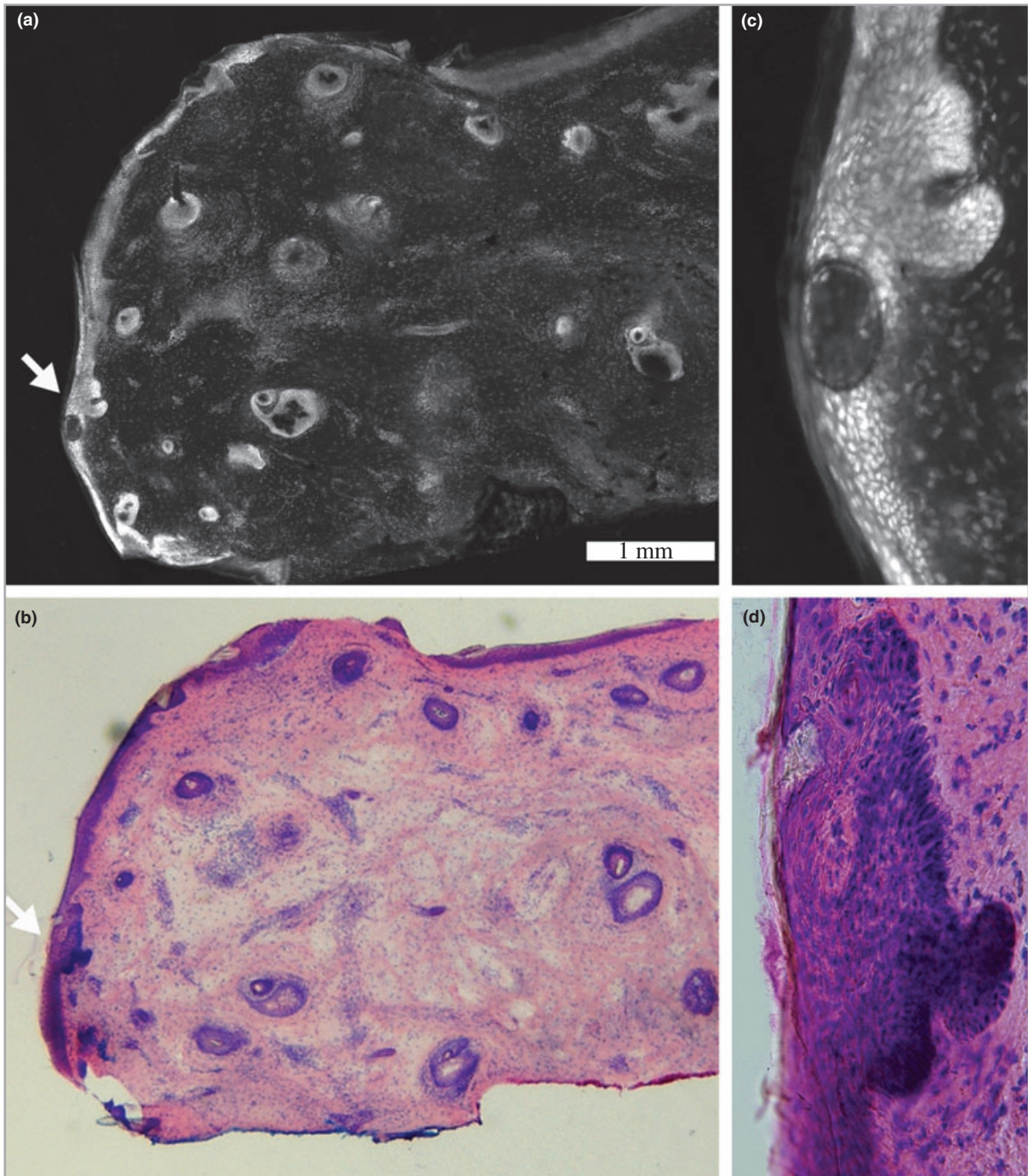


Fig 3. Fluorescent confocal submosaic (a) of a superficial basal cell carcinoma (BCC) and the corresponding haematoxylin and eosin-stained Mohs frozen section (b) at $4\times$ magnification. The bright focus (arrow) along the epidermal margin is suspicious for residual tumour. Digital zooming to higher magnification of $30\times$ reveals the subtle but characteristic features of superficial BCC, in both the confocal image (c) and the frozen section (d).

Discussion

This study demonstrates the feasibility and accuracy of fluorescent confocal mosaicing microscopy, using acridine orange for nuclear staining, to detect residual BCC of all subtypes and

differentiate from normal skin in excised tissue from Mohs surgery. The early findings of Al-Arashi *et al.*¹⁶ and our recent results suggest that standard fluorescence contrast agents may prove useful for rapid nuclear staining of excised skin tissue. These findings represent another advance in our ongoing

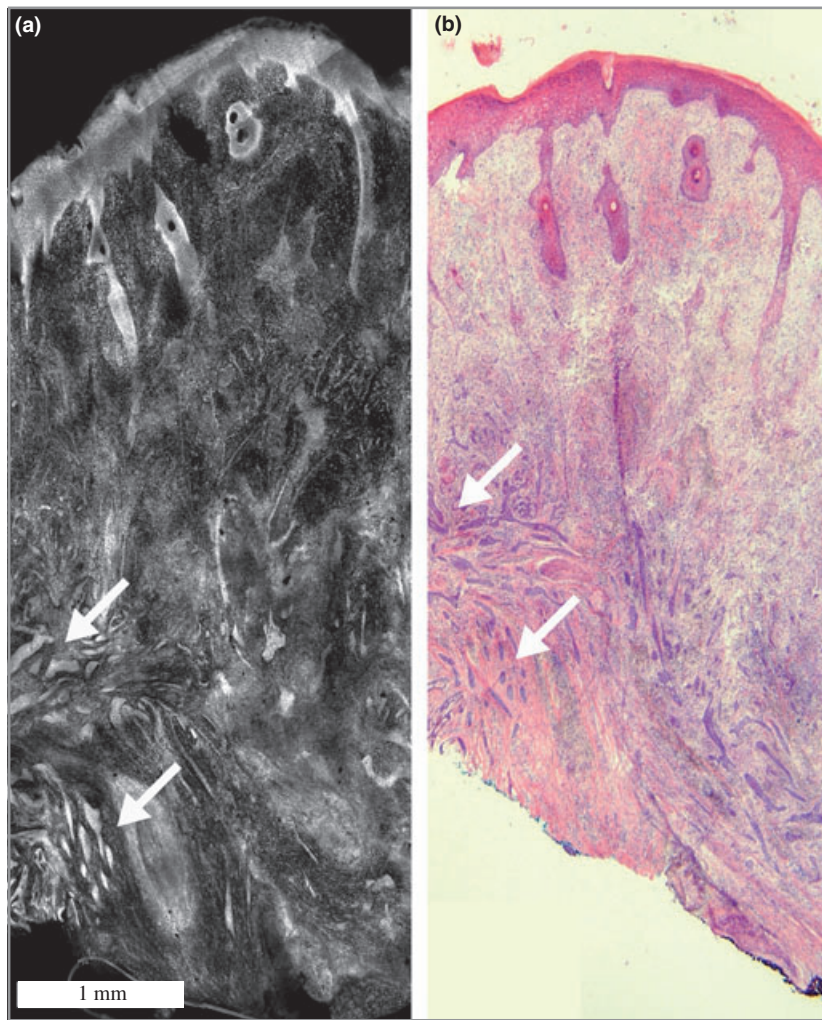


Fig 4. Fluorescent confocal submosaic (a) of residual infiltrative basal cell carcinoma (BCC) and the corresponding haematoxylin and eosin-stained Mohs frozen section (b) at 4 × magnification. The residual infiltrative BCC (arrows) is seen within the reticular dermis as bright strands in the submosaic (a) and basophilic strands in the frozen section (b). The strands are four to eight cells thick. A surrounding inflammatory infiltrate is also evident.

translational research to develop potential clinical applications for confocal microscopy. The long-term goal is rapid real-time imaging to provide surgical pathology-at-the bedside in excised skin and other tissues. Such scenarios are already being explored in the surgical arena relating to real-time interpretation of breast, parathyroid and ovarian tissues with confocal microscopy.^{18–20}

Although fluorescence confocal microscopy requires contrast agents to stain nuclear detail, this technology may offer advantages over standard pathology given rapid contrast staining within seconds and ability to view tissue pathology in real time without need for tissue processing. In contrast, traditional processing of Mohs frozen sections is labour intensive, time consuming, and accounts for ~15% of the operating costs (i.e. total of ~\$150 million per year in the U.S.A.)²¹ in Mohs surgery. In other surgical settings such as head-and-neck and breast cancers, large excised specimens may be examined rapidly leading to more accurate and complete removal of tumour associated with lower costs. Other tissues such as bone are not amenable to frozen sections but can be directly imaged with confocal microscopy.²²

The differences between the two observers' assessments may be explained based on the experience level as a Mohs

surgeon and experience with evaluating confocal images. Observer 1, a senior Mohs surgeon with approximately 10 years of experience in studying confocal images, performed with sensitivity of nearly 99%. The lower specificity of 83.3% is likely to be related to several factors. The senior Mohs surgeon was very experienced in evaluating confocal reflectance images with acetic acid during initial years of research^{11–14} but was new to the fluorescent acridine orange confocal modality. Although acetic acid and acridine orange both show bright nuclear morphology, there are intrinsic differences in the two forms of contrast. Secondly, the senior Mohs observer was deliberately conservative, as appropriate when evaluating any new technology, and thus recorded as 'positive' all suspicious foci, which included artifacts due to saturation and dense inflammation. Observer 2 is a Mohs Fellow with only a few months of experience with confocal microscopy that was acquired during this study. Several cases missed by observer 2 early in the study were likely to be due to observer 2's lack of familiarity with reading confocal images. As the study progressed, the sensitivity improved quickly, suggesting a rapid learning curve for interpreting confocal mosaics.

In general, challenges in interpreting confocal mosaics mirrored those that are routinely encountered with Mohs

pathology. The challenges included missed diagnosis of superficial BCC tumour when the epidermal margin was not fully intact, confusion of small hair follicles with BCC, and difficulty in interpreting dense inflammation. Both observers found interpretation of superficial tumour to be the most challenging, especially when the adjacent epidermal margin was incomplete. This is likely to be a result of tissue disruption as the confocal mosaics were acquired on the discarded excisions following the preparation of Mohs frozen pathology. Such distortions may be minimized when fresh tissue is imaged directly after excision. Of note, there was no difficulty in interpreting infiltrative BCCs on confocal images.

This pilot feasibility study reviewed a relatively small convenience sample ($n = 48$). Although the results are promising, they should be tempered by the limited number of observations and reviewers. To combat issues of generalizability, we enriched the sample to include all the major subtypes of BCC. However, further work needs to be done with a larger sample and multiple reviewers.

This study was performed *ex vivo* as initial feasibility studies could be performed only following completion of the Mohs procedure. The imaging was facilitated by the fact that the cryostat-sectioned margin presented a conveniently flat surface for imaging. As we advance towards imaging directly on freshly excised Mohs tissue, we anticipate challenges in mounting tissue of variable thickness, size and contour to enable visualization of the complete surgical margins.

In order for real-time confocal imaging to have true clinical utility, several factors still require improvement and further study. In our initial clinical evaluation we focused solely on confocal imaging of BCCs as they constitute 80% of all skin cancers. Although very accurate in the detection of BCCs, applicability of confocal imaging to other tumours will need to be explored as the success of Mohs surgery hinges on the ability to truly 'read tissue' – i.e. to diagnose all tumour types and benign proliferations. This may require multimodal imaging, similar to the use of multiple stains in pathology to differentiate tumour origins. For example, reflectance confocal microscopy is being combined with Raman spectroscopy for detection of BCCs,² which may enhance diagnostic accuracy but still requires further clinical study with a large sample size and advanced statistical analysis. Furthermore, to match the accuracy of conventional histology, ultimately a reproducible contrast protocol, consistent image quality, and near perfect interpretation record will be needed to meet the rigorous expectations of clinicians. Finally, further translational advances in image acquisition and mosaicing speed and availability of compact, inexpensive and user-friendly equipment will be necessary for acceptance into the clinical realm. Preliminary engineering suggests that mosaics of up to 20×20 mm may be created in 2–3 min. A recently developed commercial version (VivaScope 2500; Lucid Inc.) of our confocal mosaicing microscope occupies a footprint of 20×28 cm and costs \$50 000. Ongoing technology research in line-scanning^{23,24}

shows preliminary promise for confocal microscopes with smaller footprints (possibly 13×13 cm) and lower costs in the \$10 000 range.

Acknowledgments

We are indebted to Klaus J. Busam, MD for his help with pathology, Billy Huang for help with the mosaicing, and Zach Eastman and William Fox of Lucid Inc. for technical support. This research was funded in part by the National Institutes of Health (NIH), grant R01EB002715 from the Image-Guided Interventions program of the National Institute of Biomedical Imaging and Bioengineering, and in part by a grant from the Byrne Fund, Department of Medicine at Memorial Sloan-Kettering Cancer Center.

References

- 1 Nijssen A, Maquelin K, Santos LF *et al.* Discriminating basal cell carcinoma from perilesional skin using high wave-number Raman spectroscopy. *J Biomed Opt* 2007; **12**:034004.
- 2 Lieber CA, Majumder SK, Billheimer D *et al.* Raman microscopy for skin cancer detection. *J Biomed Opt* 2008; **13**:024013.
- 3 Yaroslavsky AN, Salomatina EV, Neel V *et al.* Fluorescence polarization of tetracycline derivatives as a technique for mapping non-melanoma skin cancers. *J Biomed Opt* 2007; **12**:014005.
- 4 Paoli J, Smedh M, Wennberg AM, Ericson MB. Multiphoton laser scanning microscopy on non-melanoma skin cancer: morphologic features for future non-invasive diagnostics. *J Invest Dermatol* 2007; **128**:1248–55.
- 5 Lin SJ, Jee SH, Kuo CJ *et al.* Discrimination of basal cell carcinoma from normal dermal stroma by quantitative multiphoton imaging. *Opt Lett* 2006; **31**:2756–8.
- 6 Galletly NP, McGinty J, Dunsby C *et al.* Fluorescence lifetime imaging distinguished basal cell carcinoma from surrounding uninvolved skin. *Br J Dermatol* 2008; **159**:152–61.
- 7 Ericson MB, Uhre J, Strandeberg C *et al.* Bispectral fluorescence imaging combined texture analysis and linear discrimination correlation with histopathologic extent of basal cell carcinoma. *J Biomed Opt* 2005; **10**:1–8.
- 8 Stenquist B, Ericson MB, Strandeberg C *et al.* Bispectral fluorescence imaging of aggressive basal cell carcinoma combined with histopathological mapping: a preliminary study indicating a possible adjunct to Mohs micrographic surgery. *Br J Dermatol* 2006; **154**:305–9.
- 9 Olmedo JM, Warschaw KE, Schmitt JM, Swanson DL. Optical coherence tomography for the characterization of basal cell carcinoma *in vivo*: a pilot study. *J Am Acad Dermatol* 2006; **55**:408–12.
- 10 González S, Gill M, Halpern AC (eds). *Reflectance Confocal Microscopy of Cutaneous Tumors*. London: Informa U.K. Ltd, 2008.
- 11 Rajadhyaksha M, Menaker G, Flotte T *et al.* Confocal examination of nonmelanoma cancers in thick skin excisions to potentially guide Mohs micrographic surgery without frozen histopathology. *J Invest Dermatol* 2001; **117**:1137–43.
- 12 Chung VQ, Dwyer PJ, Nehal KS *et al.* Use of *ex vivo* confocal scanning laser microscopy during Mohs surgery for nonmelanoma skin cancers. *Dermatol Surg* 2004; **30**:1470–8.
- 13 Patel YG, Nehal KS, Aranda I *et al.* Confocal reflectance mosaicing of basal cell carcinomas in Mohs surgical skin excisions. *J Biomed Opt* 2007; **12**:034027.

- 14 Gareau DS, Patel YG, Li Y *et al.* Confocal mosaicing in skin excisions: a demonstration of rapid surgical pathology. *J Microsc* 2009; **233**:149–59.
- 15 Gareau DS, Li Y, Huang B *et al.* Confocal mosaicing microscopy in Mohs skin excisions: feasibility of rapid surgical pathology. *J Biomed Opt* 2008; **13**:054001.
- 16 Al-Arashi MY, Salomatina E, Yaroslavsky AN. Multimodal confocal microscopy for diagnosing nonmelanoma skin cancers. *Lasers Surg Med* 2007; **39**:696–705.
- 17 Benson DM, Bryan J, Plant AL *et al.* Digital imaging fluorescence microscopy: spatial heterogeneity of photobleaching rate constants in individual cells. *J Cell Biol* 1985; **100**:1309–23.
- 18 Tilli MT, Cabrera MC, Parrish AR *et al.* Real-time imaging and characterization of human breast tissue by reflectance confocal microscopy. *J Biomed Opt* 2007; **12**:051901.
- 19 White WM, Tearney GJ, Pilch BZ *et al.* A novel noninvasive imaging technique for intraoperative assessment of parathyroid glands: confocal reflectance microscopy. *Surgery* 2000; **128**:1088–100.
- 20 Makhlof H, Gmitro AF, Tanbakuchi AA *et al.* Multispectral confocal microendoscope for *in vivo* and *in situ* imaging. *J Biomed Opt* 2008; **13**:044016.
- 21 Bialy TL, Whalen J, Veledar E *et al.* Mohs micrographic surgery versus traditional surgical excision – a cost comparison analysis. *Arch Dermatol* 2004; **140**:736–42.
- 22 White WM, Baldassano M, Rajadhyaksha M *et al.* Confocal reflectance imaging of head and neck surgical specimens: a comparison with histologic analysis. *Arch Otolaryngol Head Neck Surg* 2004; **130**:923–8.
- 23 Dwyer PJ, DiMarzio CA, Zavislan JM *et al.* Confocal reflectance theta line-scanning microscope for imaging human skin *in vivo*. *Opt Lett* 2006; **31**:942–4.
- 24 Dwyer PJ, DiMarzio CA, Rajadhyaksha M. Confocal theta line-scanning microscope for imaging human tissues *in vivo*. *Appl Opt* 2007; **46**:1843–51.